This document is currently under revision by the European Commission (EC) and has not yet been validated or approved by the EC. The content provided herein is subject to change, and the information presented may not represent the final position or official stance of the EC.

This document is being shared for informational purposes only and is not to be considered an official or authoritative source of information from the European Commission. Any decisions, actions, or interpretations based on the content of this document should be taken with caution, as the content may be subject to modification or revision by the EC.

The EC accepts no liability for any inaccuracies, errors, or omissions in this document, and any reliance on its content is at the user's own risk. It is recommended to verify the information provided in this document with official EC publications or communications before making any decisions or drawing any conclusions based on its content.

Please note that the content in this document may be confidential or sensitive in nature and should be treated as such. Unauthorized dissemination, distribution, or use of this document is strictly prohibited.

By accessing and reviewing this document, you acknowledge and accept the terms of this disclaimer.

BL2F

Transforming Black Liquor to Biofuel

Research and Innovation Action

H2020-LC-SC3-2019-NZE-RES-CC

D2.3 - Report on aqueous phase reforming concept

WP2 - Task 2.3

20th December 2023

Lead Beneficiary: VTT Technical Research Centre of Finland Ltd

Author(s): Jasmiina Palo (VTT), Sari Rautiainen (VTT), David Baudouin (PSI)
Reviewers(s): Pavel Kukula (Ranido), Ursel Hornung (KIT)

@BL2F_EU **www.bl2f.eu** **BL2F_EU**

This project has received funding from the European Union's Horizon 2020 research and innovation programme under the Grant Agreement n°884111.

Disclaimer

The content of this deliverable reflects only the author's view. The European Commission is not responsible for any use that may be made of the information it contains.

Document Information

Grant agreement	884111
Project title	Black Liquor to Fuel by Efficient Hydrothermal Application integrated to Pulp Mill
Project acronym	BL2F
Project coordinator	Prof. Dr. Tero Joronen
Project duration	1st April 2020 – 31st March 2024 (48 Months), including extension of 12 months
Related work package	WP2 - Salt recovery and side stream valorization
Related task(s)	Task 2.3 - Aqueous phase reforming
Lead organisation	VTT
Contributing partner(s)	VTT, PSI
Due date	31st December 2023
Submission date	20th December 2023
Dissemination level	Public

History

Date	Version	Submitted by	Reviewed by	Comments
18.10.2023	0	J. Palo	M. Reinikainen (VTT)	Issued for comments
26.10.2023	1	J. Palo	J. Lehtonen (VTT), S. Rautiainen (VTT), D. Baudouin (PSI)	Comments from M. Reinikainen included. Issued for comments on the APR integration possibility and task deviations
27.11.2023	2	J. Palo	P. Kukula (Ranido), U. Hornung (KIT)	Comments included, issued for review
20.12.2023	3	J. Palo		Reviewers' comments included

Table of contents

List of figures

List of tables

Abbreviations and acronyms

Acronym	Description
4MC	4-methylcatechol
AcOH	Acetic Acid
AP	Aqueous Phase
APR	Aqueous Phase Reforming
BET	Brunauer–Emmett–Teller
BL	Black Liquor
FID	Flame Ionization Detector
HDO	Hydrothermal Oxygenation
HTL	Hydrothermal Liquefaction
ICP	Inductively Coupled Plasma
IWI	Incipient Wetness Impregnation
MeOH	Methanol
TCD	Thermal conductivity detector
TEM	Transmission Electron Microscopy
TOC	Total Organic Carbon content
TOS	Time-On-Stream (min)
WGS	Water Gas Shift reaction
WHSV	Weight Hourly Space Velocity (h^{-1})
WP	Work Package
XRD	X-ray Diffraction

Executive Summary

The main objective of Task 2.3 was to study the Aqueous Phase Reforming (APR) of the black liquor-based aqueous phase, specifically the liquid product from Hydrodeoxygenation (HDO) of a fluidized black liquor, to produce hydrogen for the HDO step of the BL2F process. To achieve this goal, an extensive catalyst screening process was carried out using four individual model compounds to study the activity and stability of catalysts. The model compounds used in the study were methanol, acetic acid, phenol, and 4-methylcatechol, which were selected based on the analytical results from the Hydrothermal liquefaction (HTL) studies done at KIT for Task 1.2 and reported in D1.2. VTT synthesized 4 nickel and iron-based catalysts and compared their behavior against two commercial noble metal catalysts. Based on the results of the screening phase, the two best catalysts were studied with a more realistic mixture of the four model compounds in a long-term experiment.

The nickel catalysts were found to be more selective to hydrogen than noble metal catalysts, but they deactivated quickly due to catalyst fouling, or metal leaching with acetic acid. On the other hand, the noble metal catalysts were found to be more stable in the tested conditions, however, their selectivity to targeted hydrogen is decreased due to the consumption of produced H_2 in side reactions involving liquid organics (e.g. hydrogenation). Overall, the study revealed that significant improvements are needed to enhance catalysts' stability and selectivity for larger scale hydrogen production. For future work, the authors propose two studies, with a focus on improving resistance towards deactivation (coking) on one side, and on the other side studying the effect of other parameters of the process water, including pH, sulfur, and remaining salts, using more complex model solutions and real process feed.

Keywords

Black liquor, Fuel, Aviation, Shipping, Aqueous-phase reforming, APR

1 Introduction

The BL2F project is focused on developing an innovative technology that can convert black liquor (BL) into synthetic drop-in fuels. The process (Figure 1) involves conversion of wet BL into biocrude using a combination of salt-separation and hydrothermal liquefaction (HTL). This biocrude is then upgraded through a two-steps hydrodeoxygenation (HDO) process, a first hydrothermal HDO followed by a conventional one, to reduce the oxygen content of the resulting oil. To increase conversion efficiency, aqueous streams from HTL and HDO are valorised using aqueous phase reforming (APR) to produce H_2, which can be utilized as a supply for HDO processes. APR is a catalytic process that can produce hydrogen and carbon dioxide from oxygenated compounds in liquid phase (Coronado et al., 2018; Davda et al., 2003; Pipitone et al., 2022). To keep the solution in liquid form, APR reactions are typically carried out at temperatures (220 – 270 °C) and moderate pressures (30 – 60 bar), thus providing also economic benefits by eliminating the need for feed vaporization.

In Task 2.3, the aim was to investigate hydrogen production from HTL-oil aqueous streams via catalytic APR at laboratory scale. The main tasks included screening of several catalysts with simulated aqueous phase (AP), and a study of the best catalysts from screening in a long-term operation using an actual BL-based aqueous phase from the HDO. Moreover, experimental results were used to further assess the integration possibility of APR to BL2F process concept.

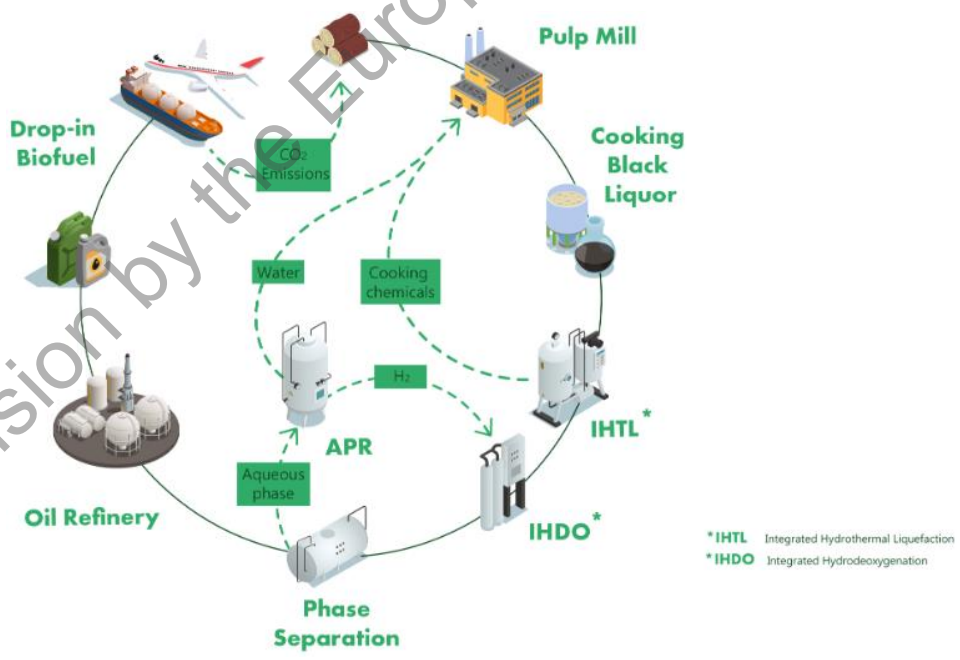

Figure 1. Concept overview for BL2F project.

2 Experimental: Aqueous-phase reforming of black liquor derived water

This section describes the feedstock, catalysts preparation, characterization methods, laboratory-scale test unit, and experimental conditions used.

2.1 Feedstock

Based on the BL2F process concept, the aqueous phase separated after the hydrothermal HDO of the BL HTL-product would undergo APR to produce hydrogen for the HDO process. During the course of the project, TAU encountered significant technical difficulties at the HTL-plant and as a result, the delivery of BL-based HTL aqueous phase was severely delayed and ultimately unavailable for the APR tests in the required amounts and timeline. This meant that our work in Task 2.3 was limited to conducting experiments with simulated feedstock. To estimate the composition of real APR feed, we used model components and carbon concentration based on the analysis of the HTL-products produced in the batch experiments at KIT (D1.2, Task 1.2) where real BL was used as a reactant. It's important to note that the HTL plant at TAU was designed to extract the salts in a separate brine stream, producing a desalinated stream composed of the biocrude and the aqueous phase of interest for APR. However, in the batch tests in this deliverable, no salt separation was performed, yielding a unique liquid product that might differ from the continuous process.

According to D1.2, the main compounds found in the liquid sample produced from HTL of BL were carboxylic acids (acetic acid and formic acid), hydroxy acids (glycolic acid and lactic acid), light alcohols (methanol and ethanol), along with dissolved oxygenated aromatics such as catechol, 4-methylcatechol, phenol, guaiacol, and syringol. For our work, we selected methanol, acetic acid, phenol, and 4-methylcatechol as the model compounds to represent the main functionalities of different chemical groups. We studied each model compound individually and later in a mixture containing all four components. All model compound mixtures were prepared using deionized water with a total organic carbon content of 5-10 wt.%. Table 1 displays the studied model compound mixtures, their corresponding concentrations, and measured pH. In the following chapters, the model compound mixtures will be further addressed with their given abbreviations listed in Table 1.

Table 1. Selected APR model compounds, concentrations of the prepared solutions, and measured pH

Compound(s)	Abb.	Conc.(wt%)	pH	Structure
Methanol	MeOH	5	6.7	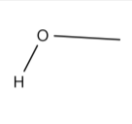
Acetic acid	AcOH	5	2.5	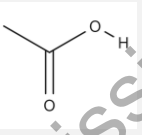
Hydroxybenzene	Phenol	5	4.1	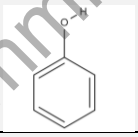
4-methylcatechol	4MC	5	3.9	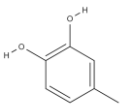
Methanol Acetic acid Hydroxybenzene 4-methylcatechol	MIX-4	2.5 2.5 2.5 2.5	2.8	

2.2 Catalysts and catalyst preparation

2.2.1 Selection of APR catalysts

Six different catalysts were selected to be studied for APR of BL waters. Out of these catalysts, three nickel and one iron catalyst were prepared at VTT. Nickel catalysts were selected based on their high activity and good selectivity to hydrogen production, as demonstrated in our previous work on aqueous-phase reforming of biorefinery water fractions (Coronado et al. 2017, 2018). However, nickel catalysts are known to have issues with deactivation, especially when using sulfur-containing feedstocks. Therefore, we also tested a Fe catalyst which is presumably less sensitive to sulfur under these conditions (Baudouin et al., 2022) to compare the catalyst stability and performance. Moreover, iron catalysts are known for their good Water Gas Shift (WGS) activity, which is one of the desired reactions in APR. Additionally, we selected two commercial noble metal catalysts, Pt/AC and Ru/AC, as benchmark materials, out of which Ru was chosen to be studied in sulfided form (RuS_x/AC) to evaluate the catalyst's activity in its poisoned form. Compared to base metals, noble metals are often used for APR and other liquid phase reactions despite their moderate selectivity to H_2, because of their better hydrothermal stability, particularly at low pH. Furthermore, the stability under hydrothermal conditions was

also considered when choosing suitable support materials. Table 2 provides details of the selected catalysts, including their compositions, manufacturers, and information on their pre-treatment methods. Each catalyst was given a specific ID code for easy reference in the discussion of the results.

Table 2. List catalysts selected for catalyst screening

ID	Active metals	Support	Target active metal loading (wt.%)	Manufacturer	Pretreatment procedure
NiCu/Ce-Zr	Ni-Cu	0.25CeO_2 0.75 ZrO_2	10 Ni, 5 Cu	VTT (IWI)[a]	*In-situ* reduction: 2 h, 450 °C, 1 bar, H_2:N_2=1, 150 cm^3/min
NiCu/Al	Ni-Cu	γ-Al_2O_3	10 Ni, 10 Cu	VTT (IWI)[a]	*In-situ* reduction: 2 h, 450 °C, 1 bar, H_2:N_2=1, 150 cm^3/min
NiCo/ZrO_2	Ni-Co	ZrO_2	10 Ni, 5 Co	VTT (IWI)[a]	*In-situ* reduction: 2 h, 450 °C, 1 bar, H_2:N_2=1, 150 cm^3/min
Fe/SiO_2	Fe-Co-K	SiO_2	15 Fe, 2 Cu, 0.5 K	VTT (IWI)[a]	*In-situ* reduction: 2 h, 500 °C, 1 bar, H_2:N_2=1, 150 cm^3/min
Pt/AC	Pt	Activated carbon	5 Pt	NOBLYST®, Sigma-Aldrich	*In-situ* reduction: 2 h, 250 °C, 1 bar, H_2:N_2=1, 150 cm^3/min
RuS_x/AC*	Ru	Activated carbon	5 Ru	Ranido, RCAT-8830	*Ex-situ* sulfidation using DMDS. Sulfidation done in autoclave at following conditions: 4 h, 325 °C, 30 bar (H_2), hexane used as solvent (hexane:DMDS=21)

[a] Incipient wetness impregnation (IWI), catalysts prepared at VTT
* Sulfided catalyst

2.2.2 Benchmark materials

Two noble metal catalysts were acquired for catalyst testing. The 5 wt.% Pt/AC catalyst (NOBLYST®) was provided by Sigma-Aldrich, and the 5 wt.% Ru/AC (RCAT-8830) catalyst was supplied by Ranido. On the contrary to the other catalysts, Pt/AC was supplied in a very fine powder, and to prevent reactor blockage during operation, e.g., due to catalyst fouling, and avoid preferential pathways, it was diluted with inert SiC (0.15-0.21 mm) with 1:1 volume ratio.

2.2.3 Materials for nickel and iron catalyst preparation

Supports used for nickel catalysts were ZrO_2 (Accusphere® 0.5mm, Saint-Gobain), γ-Al_2O_3, (Accusphere® 0.5mm, Saint-Gobain), and CeO_2-ZrO_2 (powder form, MEL Chemicals). Iron was supported on SiO_2 (3 mm) obtained from Saint-Gobain. The metal precursors, nickel(II) nitrate hexahydrate ($Ni(NO_3)_2 \cdot 6H_2O$, 99.999%), cobalt(II) nitrate hexahydrate ($Co(NO_3)_2) \cdot 6H_2O$, 98%), and copper(II) nitrate trihydrate ($Cu(NO_3)_3 \cdot 3H_2O$, 103%), $Fe(NO_3)_3 \cdot 9H_2O$, and KNO_3 were supplied by Sigma-Aldrich.

2.2.4 Preparation of catalysts

Four different catalysts, three Ni-based and one Fe-based catalyst were prepared at VTT using incipient wetness impregnation (IWI). The nickel catalysts followed the recipe described in Coronado et al. (2018). ZrO_2 and γ-Al_2O_3 supports were used as received, while the CeO_2-ZrO_2 support was calcined at 450 °C for 10 h in flowing air, pelletized, crushed, and sieved to 0.2-0.3 mm prior to metal impregnations. The nickel catalysts were prepared by co-impregnation of nickel and copper or cobalt precursors in aqueous solutions. After impregnation of the metal precursors, the catalyst was kept at room temperature overnight, followed by drying at 80 °C and calcination under flowing air at 500 °C for 4 hours.

In case of the Fe catalyst, SiO_2 support was crushed and sieved to 0.1-0.2 mm particles before metal impregnations. To attain targeted metal concentrations, iron, cobalt and potassium were co-impregnated twice on the SiO_2 support. Between impregnations, the catalyst was kept at room temperature for 24 hours, followed by drying at 80 °C. After repeating these steps twice, the catalyst was calcined under flowing air at 400 °C for 4 hours.

2.3 Catalyst characterization

Self-made nickel catalysts were characterized extensively with the following methods: nitrogen adsorption and desorption, X-ray diffraction (XRD), inductively coupled plasma optical emission spectroscopy (ICP-OES), transmission electron microscope (TEM), and for their carbon content. Data is reported also for the other catalysts when available.

Nitrogen ADS-DES procedure

Nitrogen physisorption was performed with a Micromeritic 3Flex equipment. Before the analysis, the catalysts were degassed in high vacuum for 19 hours at 200 °C. Degassing of spent catalyst samples was performed at 120 °C for minimum 5 hours to prevent detachment of plausible carbon species from the catalyst surface. For carbon supported catalysts, that typically can adsorb a lot of water into their micropore structure, the degassing time was extended to overnight.

XRD procedure

X-ray diffraction (XRD) was conducted with Panalytical X´pert Powder with Cu K α 1 radiation (45 kV and 40 mA) with continuous scanning from 20° to 110° 2 θ with step size of 0.0131°. Analysis was done by using Panalytical HighScore Plus 4.0 software. The crystallite size of catalyst particles was calculated with Scherrer equation (Eq 1.). The wavelength (λ) of Cu K- α applied in the Scherrer equation was 1.541874 Å and the crystallite shape factor (K) was 0.9. Catalysts were measured as received.

$$\tau = \frac{K\lambda}{\beta_\tau \cos\theta} \qquad \text{(Eq. 1)}$$

ICP-OES procedure

The metal loadings, Co, Cu, and Ni, of fresh and spent catalysts were analyzed using ICP-OES (5110 SVDV, Agilent Technologies). The samples were analyzed as received. For the analysis, 200 mg of catalyst sample was dissolved with microwave assisted acid digestion in the presence of concentrated HNO_3 and HCl solutions at temperature of 180 °C, and were further diluted with 1 % nitric acid solution (EMPLURA ®).

TEM procedure

Transmission electron microscopy (TEM) was performed on a probe corrected JEOL JEM-ARM200F (NeoARM) microscope equipped with a cold field emission gun operated at 200 keV and a OneView CMOS camera (IS-version; Gatan). It was also used for STEM and EDX investigations, for which a JEOL EDX detector "Centurio 100" was used to measure the elemental composition.

Carbon content analysis

Carbon content analysis was done for fresh and spent catalysts with LECO CHN 828 analyzer by burning the sample with pure oxygen at 950 °C. The samples were analyzed as received.

2.4 Test unit

APR set-up was designed and constructed by VTT Technical Research Centre of Finland (Figures 2 and 3). APR experiments were conducted using a continuous tubular stainless-steel reactor (L=400 mm, ID 8 mm) with downward flow. The set-up was equipped with Bronkhorst mass flow controllers to supply N_2 and H_2 gases. Nitrogen was used for pressurization, purging, diluting H_2 during catalyst reduction in-situ, and was co-fed with aqueous phase during APR experiments to aid desorption of the gaseous products from the liquid phase. The AP was fed with a HPLC pump (Knauer P 4.1S) that has a flow rate range of 0.01 – 10 cm^3/min and can pump to pressures up to 150 bar. The system pressure was controlled with a back-pressure regulating valve located in the reactor outlet.

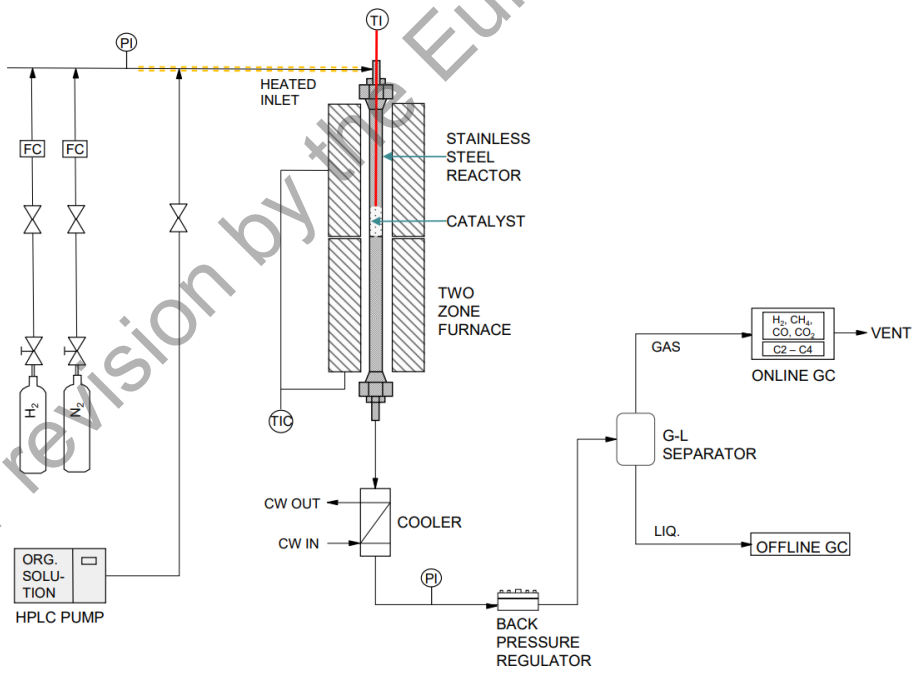

Figure 2. Scheme of the APR test set-up at VTT.

Figure 3. Picture of the experimental set-up at VTT.

2.5 Execution of the APR experiments

For each experiment, 1.5 g of a catalyst was packed into the middle of the reactor. The catalyst was poured on top of a metal grate covered with a small amount quartz wool to prevent catalyst moving downstream. The reactor was placed inside an oven capable of heating up to 600 °C and connected to the line. Prior to each experiment, the reactor was pressure tested up to 30 bar for safety. After the pressure test, the catalyst was reduced in-situ with H_2:N_2=1 flow of 150 cm^3/min for two hours. The reduction temperature used for each catalyst can be found in Table 2, except for Ru/AC catalyst, which was used in its sulfided form, as received, without additional pre-treatments. After the catalyst reduction, the system was flushed with nitrogen until no H_2 was detected in the micro-GC. Next, the reactor was pressurized for 32 bar(g) with nitrogen and the catalyst bed temperature was set to 230 °C. Once the reaction conditions were met the liquid feed with a flow rate of 2 cm^3/min was introduced to the system via heated line (150 °C). In addition, N_2 was co-fed through the reactor with a flow of 75 Ncm^3/min during the experiment and used as an internal standard for evaluating the composition of gaseous products. Experiments were carried out for three hours after the desired operation conditions were reached. After the experiment, pumping of the AP was stopped and the catalyst was dried overnight at 150 °C with N_2 flow before disassembling the reactor. As a baseline, we conducted a test with no catalyst, for each model solution. The blank tests followed a similar procedure to the catalyst screening. The detected H_2 content at the outlet gas was found to be less than 0.004 vol-% for all model compounds without any evidence of conversion of the organics during the blank tests.

2.6 APR sample analytical methods

Gaseous products were analysed online using a four-channel Agilent 490 Micro GC that included CP-Molsieve 5A, CP-PoraPlot U, CP-Al_2O_3/KCl, and CP-Sil 5CB columns with four TCDs (Thermal conductivity detector). Liquid products were collected from the gas-liquid separator every 30 min and analysed offline with a Shimadzu GC-2010 Plus equipped with a HP-INNOWax column (60 m x 0.25 mm x 0.25 µm) and a flame ionization detector (FID). 2-Butanol was used as an internal standard. The compounds were quantified by taking the average of three parallel GC samples. The analysis program was as follows: temperature was held at 60 °C for 3 min, then increased to 230 °C with the heating rate of 10 °C/min and hold at that temperature for 30 min. We note that the liquid products were always collected as a single phase, i.e., no 2nd liquid phase was detected in any of the experiments. Additionally, there were small solid residues in some liquid samples, most likely originating from the catalyst.

2.7 Calculation methods

The catalysts performance was evaluated based on model compound conversion (X_j, Eq. 2), product selectivity (S_i, Eq. 3), hydrogen production rate (H_2Pr, Eq. 4), hydrogen yield (Y_{H_2}, Eq. 5), and H_2/CO_2 ratio (Eq. 6). Carbon balance (CB) closure was calculated using equation 7.

$$X_j(\%) = \frac{x_{j,in} - x_{j,out}}{x_{j,in}} \cdot 100 \quad \text{(Eq. 2)}$$

$$S_i(\%) = \frac{\dot{n}_{i,out}}{\sum I} \cdot 100 \quad \text{(Eq. 3)}$$

$$H_2\,Pr\ (\mu mol/min \cdot g_{cat}) = 10e^6 \cdot \frac{\dot{n}_{H_2}}{m_{cat}} \quad \text{(Eq. 4)}$$

$$Y_{H_2}(\%) = \frac{\dot{n}_{H_2}}{\dot{n}_{j,in}} \cdot 100 \quad \text{(Eq. 5)}$$

$$H_2/CO_2\ ratio = \frac{\dot{n}_{H_2}}{\dot{n}_{CO_2}} \quad \text{(Eq. 6)}$$

$$CB\ (\%) = \frac{\dot{n}_{c,out}}{\dot{n}_{c,in}} \cdot 100 \quad \text{(Eq. 7)}$$

In Eq. 2, *j* refers to the model compound used in the simulated AP and x is the mass fraction of the model compound. In Eq. 3 – 7 $\dot{n}$ is the molar flow rate expressed in mol/min, *i* is used for the reaction products for both gas and liquid phase, and m_{cat} is the mass of the catalyst.

3 Results

3.1 Characterization of fresh catalysts

In this work, we focused on the characterization of self-prepared nickel catalysts. The catalysts were analyzed using various methods such as ICP-OES, XRD, TEM, and N_2 physisorption to determine their textural properties. Table 3 summarizes the data obtained from ICP, XRD, and N_2 physisorption. The BET surface areas of the supports ranged from 95 m^2/g (ZrO_2) to 230 m^2/g (γ-Al_2O_3). After metal impregnation, the surface areas and pore volumes decreased for all fresh catalysts, except for the $NiCo/ZrO_2$ catalyst, which maintained a similar pore volume before and after metal loading. The average pore diameter remained within the error of the analysis for all catalysts after Ni and promoter impregnation. According to ICP, NiCu/Ce-Zr and $NiCo/ZrO_2$ catalysts successfully reached their target loadings of 10 wt.% of nickel and 5 wt.% of promoters. However, for NiCu/Al, the target values of 10 wt.% Ni and 10 wt.% Cu were not entirely met. The crystal size of the reduced catalysts (mixed alloy) was calculated from X-ray diffractograms using the Scherrer equation (Eq 1). NiCu/Ce-Zr had the largest crystallite size of 27 nm, followed by Al and ZrO_2 with 18 and 17 nm crystal size, respectively. When comparing the pore sizes for different supports, the results indicate that most of the active metal particles were most likely located outside the pores as rather large clusters.

Table 3. Metal contents (ICP-OES), crystallite size (XRD analysis), and textural properties of nickel catalyst and catalyst supports (N_2 physisorption)

		ICP-OES		XRD	N_2 physisorption		
		Ni (wt.%)	Cu or Co (wt.%)	$d_{mixed\ alloy}$ (nm)[a]	S_{BET} (m^2/g)	V_p (cm^3/g)[b]	d_p (nm)[c]
Ce-Zr	support	-	-	-	134	0.28	7.1
NiCu/Ce-Zr	fresh	10.7	4.9	27	88	0.19	7.4
Al	support	-	-	-	230	0.59	10.0
NiCu/Al	fresh	8.1	6.2	18	184	0.53	10.2
ZrO_2	support	-	-	-	95	0.23	8.8
$NiCo/ZrO_2$	fresh	9.6	4.2	17	63	0.23	11.2

[a] Crystallite size of nickel-promoter species by XRD for reduced sample
[b] Pore volume calculated by BJH desorption isotherm for calcined sample
[c] Average pore diameter by BJH desorption for calcined sample

Table 4 contains the characterization data for noble metal and Fe catalysts. Fe catalyst was analysed for its metal loading and textural properties. Pt catalyst was analyzed by N_2 physisorption and for Ru, only data attainable from the manufacturer was included in the table.

Table 4. Metal contents and textural properties of fresh Pt, Ru and Fe catalyst

	ICP-OES			N_2 physisorption		
	Pt/Fe/Ru (wt.%)	Cu (wt.%)	K	S_{BET} (m^2/g)	V_p (cm^3/g)[a]	d_p (nm)[b]
Pt/AC	NA	NA	NA	915	0.43	5.4
RuS_x/AC	4.8*	NA	NA	NA	NA	NA
Fe/SiO_2	15.0	2.2	0.5	196	0.73	14.7

NA = not available
* Determined by XRF (value from manufacturer)
[a] Pore volume by BJH desorption isotherm
[b] Average pore diameter by BJH desorption

3.2 Catalyst screening

This work included an extensive catalyst screening to find the best candidate for APR of BL derived aqueous phase. In total, 45 experiments were conducted during the project, including a catalyst screening with 1-component solutions and 8 h experiments with 4-component mixture. The main results are summarized in Table 5 and will be discussed in more detail in the following chapters. We note that catalysts that did not show any activity under tested conditions were not included in the table.

Table 5. Carbon balance, H_2 production rate, product selectivity, H_2 yield, H_2/CO_2 ratio, and model compound conversion after 3 h time-on-stream in the APR of individual model compounds and 4-component mixture. Reaction conditions: 32 bar, 230 °C, $Q_{tot,liq.}$= 2 cm^3/min, m_{cat}= 1.5 g (WHSV= 4 h^{-1}), Q(N_2)=75 Ncm^3/min. ***Table continues on the next page***

Model compound	Catalyst	CB (%)	H_2Pr. (µmol/min*g_{cat})	S(H_2) (%)	S(CH_4) (%)	S(CO) (%)	S(CO_2) (%)	S(HCs) (%)	$S_{liq.}$ (%)	Y(H_2) (%)	H_2/CO_2 ratio	X_j (%)
MeOH (5 wt.%)	NiCu/Ce-Zr	101.3	642.7	76.8	0.1	0.4	22.8	0	-	33.1	3.4	8.7
	NiCu/Al	99.9	618.6	77.4	0	0	22.6	0	-	30.4	3.4	8.6
	NiCo/ZrO_2	101.2	572.2	67.8	9.2	0.9	21.4	0.7	-	29.0	3.2	12.9
	Pt/AC	100.4	657.7	76.8	0.8	0	22.4	0	-	33.5	3.4	9.7
	RuS_x/AC*	98.9	52.1	77.4	2.4	0	20.2	0	-	2.5	3.8	1.9
phenol (5 wt.%)	NiCu/Ce-Zr	Deact.	Deact.	Deact.	Deact.	Deact.	Deact.	Deact.	Deact.	Deact.	Deact.	Deact.
	NiCu/Al	Deact.	Deact.	Deact.	Deact.	Deact.	Deact.	Deact.	Deact.	Deact.	Deact.	Deact.
	NiCo/ZrO_2	99.3	14.3	66.3	0	0	28.3	0	5.4	2.1	2.3	1.8
4MC (5 wt.%)	NiCu/Ce-Zr	97.5	1.1	87.3	0	0	0	0	12.7	0.23	-	2.6
	NiCu/Al	Deact.	Deact.	Deact.	Deact.	Deact.	Deact.	Deact.	Deact.	Deact.	Deact.	Deact.
	NiCo/ZrO_2	98.2	0.2	42.3	0	0	48.3	0	9.5	0.03	0.9	1.9
	Pt/AC	97.3	1.9	27.9	0	0	19.8	0	52.3	0.36	1.4	3.6

* Sulfided catalyst

Deact. = full catalyst deactivation within testing period

Table 5. Carbon balance, H_2 production rate, product selectivity, H_2 yield, H_2/CO_2 ratio, and model compound conversion after 3 h time-on-stream in the APR of individual model compounds and 4-component mixture. Reaction conditions: 32 bar, 230 °C, $Q_{tot,liq.}$= 2 cm^3/min, m_{cat}= 1.5 g (WHSV= 4 h^{-1}), Q(N_2)=75 Ncm^3/min

Model compound	Catalyst	CB (%)	H_2Pr (µmol/min*g_{cat})	S(H_2) (%)	S(CH_4) (%)	S(CO) (%)	S(CO_2) (%)	S(HCs) (%)	$S_{liq.}$ (%)	Y(H_2) (%)	H_2/CO_2 ratio	X_j (%)
AcOH (5 wt.%)	NiCu/Ce-Zr	99.6	0.7	84.6	0	0	15.4	0	-	0.07	5.5	0.48
	NiCu/Al	Deact.	Deact.	Deact.	Deact.	Deact.	Deact.	Deact.	Deact.	Deact.	Deact.	Deact.
	NiCo/ZrO_2	Deact.	Deact.	Deact.	Deact.	Deact.	Deact.	Deact.	Deact.	Deact.	Deact.	Deact.
	Pt/AC	109.3	7.3	3.2	52.3	0	44.6	0	-	0.7	0.07	10.6
MIX-4 (2.5 wt.% of each model compound in water solution)	NiCo/ZrO_2	97.2	17.4	77.7	0	0	20.2	0	2.1	0.8	3.9	X_{MeOH}= 2.1% X_{phenol}= 1.5% X_{4MC}= 3.9% X_{AcOH}= 2.1%
	Pt/AC	90.4	57.8	20.2	1.6	0	39.4	0	38.8	2.6	0.5	X_{MeOH}= 12.6% X_{phenol}= 30.7% X_{4MC}= 70.0% X_{AcOH}= -2.8% [a]

Deact. = full catalyst deactivation within testing period

[a] More acetic acid is formed during the reaction compared to the feed concentration

3.2.1 Methanol

Methanol was used as the first model compound to represent the small alcohols present in the HTL-products. Furthermore, it is very commonly used model compound in APR studies. Six catalysts were tested for the APR of methanol in the reaction conditions described in the Section **2.5 Execution of the APR experiments**. Figure 4 shows the evolution of the methanol conversion with time on stream for each catalyst during the 3 h of test run. Fe/SiO_2 was excluded from the graph as it had no activity under tested conditions. During the methanol experiments, a reasonably stable conversion was reached throughout the testing period. After three hours on-stream (TOS=180 min), nickel and Pt catalysts exhibited a methanol conversion of approximately 10%. RuS_x/AC, on the other hand, had a stable conversion that was only about 20% of the value for nickel and Pt catalysts, showing remarkable performance for a fully sulfided (poisoned) catalyst. $NiCo/ZrO_2$ catalyst showed slightly higher activity reaching up to ~18% conversion during the first 2.5 hours, but the activity suddenly dropped to around the same level as of the other catalysts at TOS=180 min.

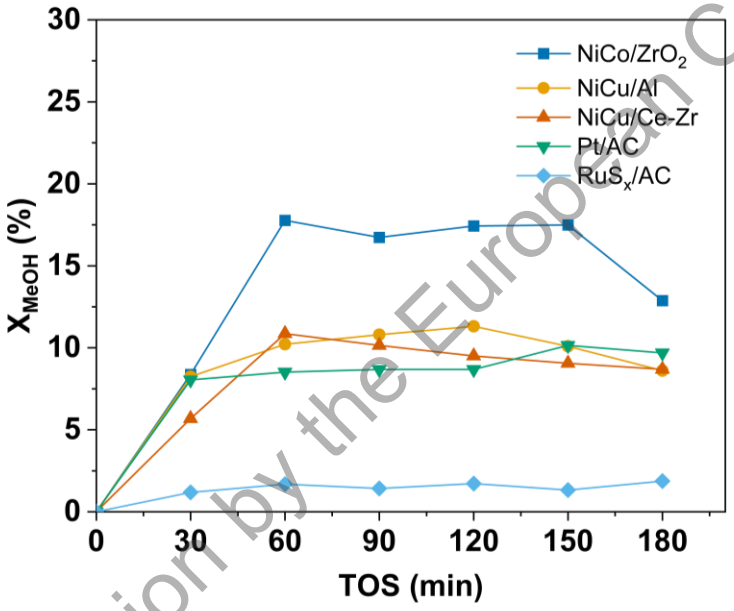

Figure 4. MeOH conversion vs. time-on-stream. Reaction conditions: 32 bar, 230 °C, $Q_{tot,liq.}$= 2 cm^3/min (5 wt.% MeOH), m_{cat}= 1.5 g, Q(N_2)=75 Ncm^3/min.

The graph in Figure 5 shows the gas phase product selectivities (S_i) as well as hydrogen production per gram of catalyst for different catalysts. The values are given at a time-on-stream of 180 minutes. No liquid products, other than unreacted methanol, were detected with any of the tested catalysts. The NiCu/Al catalyst showed the best selectivity towards targeted reaction products, H_2 and CO_2, with no other gaseous products detected. The hydrogen selectivity was around 77%, with a hydrogen production rate of 620 µmol/min•g_{cat} for the alumina-supported nickel catalyst. The $NiCo/ZrO_2$ catalyst showed the best methanol conversion, but was the least selective, with other reaction products including methane, carbon monoxide, and ethane being formed. The formation of hydrocarbons indicates that side reactions are taking place. Carbon monoxide (CO) is an intermediate product from reforming that has not reacted to CO_2 via WGS reaction. The selectivity of the two noble metal catalysts is quite similar, both showing good selectivity to hydrogen, CH_4 being a minor reaction product. However, the main difference lies in the hydrogen production. The RuS_x/AC catalyst showed significantly lower H_2 production (52

μmol/min•g_{cat}) compared to the Pt and Ni catalysts, which yet is higher than expected for a fully sulfided (poisoned) catalyst.

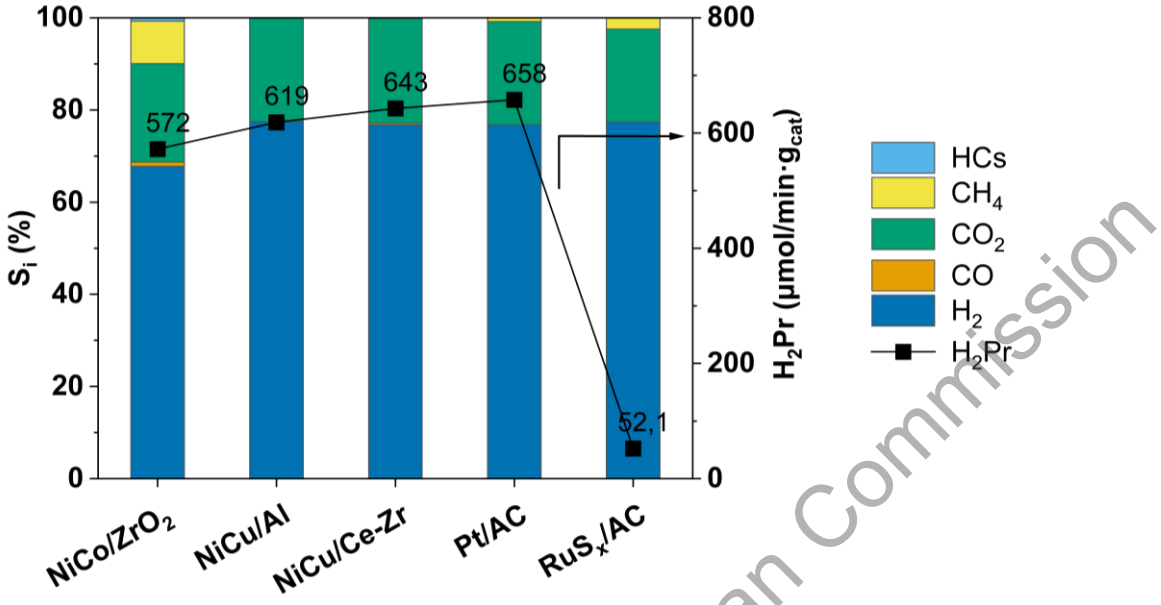

Figure 5. Product selectivity (S_i) and H_2Pr for different catalysts during MeOH APR. Reaction conditions: 32 bar, 230 °C, $Q_{tot,liq.}$= 2 cm^3/min (5 wt.% MeOH), m_{cat}= 1.5 g, Q(N_2)=75 Ncm^3/min. Reported values are at TOS= 3h.

3.2.2 4-Methylcatechol

4-methylcatechol was chosen as one of two oxygenated aromatics to be studied in APR conditions based on its presence in the HTL-product from black liquor. Based on the experimental results from the APR of methanol, we chose to study only iron, platinum, and three nickel catalysts with 4MC, as the activity with RuS_x/AC was remarkably lower than the other catalysts.

Overall, with 4MC, the hydrogen production was significantly lower compared to the experiments conducted with methanol, and a fast catalyst deactivation was observed with nickel catalysts. Thus, to compare the activity of the different catalysts, instead of conversion we looked at the hydrogen production as a function of time on stream. There was a momentary increase in H_2 production at TOS=30 min with all the three tested Ni catalysts, but the production decreased rapidly from the beginning of the test, as shown in Figure 6. On the contrary, the commercial Pt showed a low but stable H_2 production during the three-hour testing period. A steady state value of 1.9 μmol of H_2/min•g_{cat} was reached after 60 minutes with Pt/AC catalyst, with an apparent induction period in the first hour of the test. Iron catalyst did not exhibit any catalytic activity in the conditions tested and was therefore not added to the figure.

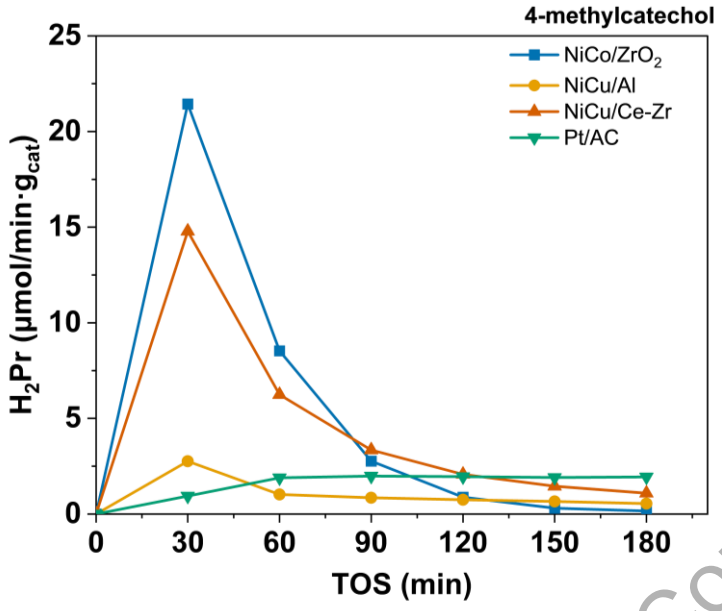

Figure 6. H_2Pr vs. time-on-stream for tested Pt and Ni catalysts in APR of 4MC. Reaction conditions: 32 bar, 230 °C, $Q_{tot,liq.}$= 2 cm^3/min (5 wt.% 4MC), m_{cat}= 1.5 g, $Q(N_2)$=75 Ncm^3/min.

In the experiments with 4MC, only CO_2 and H_2 were detected in the gas phase for all catalysts. Also, liquid products were formed, which were analyzed both with GC-MS (qualitative) and GC-FID (quantitative) methods. Quantification of the reaction products was limited to compounds that were clearly visible and properly separated in the GC chromatograms. The liquid products found in the 4MC runs were *m*-cresol, *p*-cresol, and 4-methylguaiacol. Product composition varied depending on the tested catalysts and time-on-stream. Because of the lower activity and of the catalyst deactivation, the product composition for each catalyst was compared at TOS=30 min and 180 min. In that way, we could take a closer look at possible reactions occurring at different stages of the experiment for each catalyst. The results are presented in Figure 7.

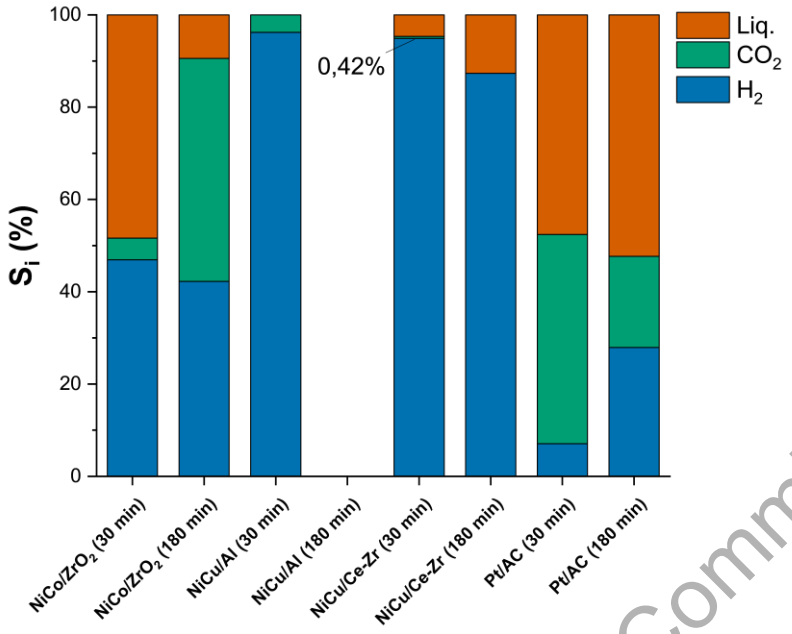

Figure 7. Product selectivity (S_i) at TOS=30 and 180 minutes during APR of 4MC. Reaction conditions: 32 bar, 230 °C, $Q_{tot,liq.}$= 2 cm^3/min (5 wt.% 4MC), m_{cat}= 1.5 g, Q(N_2)=75 Ncm^3/min.

For NiCu/Al, only CO_2 and H_2 (no liquid products) were detected during the testing period. CO_2 disappeared after 30 minutes indicating coking in phase with catalyst deactivation. At TOS=180 min, Al-supported nickel was fully deactivated (Figure 7). For NiCo/ZrO_2, the initial liquid product selectivity was notably higher compared to the one at TOS=180 min. At the same time, the CO_2 selectivity rose significantly between 30 min and 180 min. Both observations are indicating a favored initial hydrogenation of organic compounds on the fresh catalyst. With NiCo/ZrO_2, the main liquid products were *m*- and *p*-cresol.

Commercial platinum catalyst showed the highest liquid product selectivity out of the tested catalysts, with a very low hydrogen yield. This might indicate that Pt is active towards partial hydrogenation of organic compounds. Interestingly, for NiCu/Ce-Zr catalyst, at TOS=3 h, the only products were H_2 and cresols, which indicates that there is no reforming reaction occurring that could produce H_2, but rather consume H_2. There is a momentary production of CO_2 at TOS=30 min, but the product disappears shortly after that. We also noticed that the liquid product selectivity seemed to increase with NiCu/Ce-Zr towards the end of the run. This made us question the source of H_2, as the product composition did not indicate that any reforming reactions occurred. Therefore, after a set of experiments with 4MC, we also conducted experiments with pure milli-Q water with all the studied catalysts. This was to test whether the detected H_2 in the outlet originated from the reactant itself and the cause of hydrogen disappearing was due to catalyst deactivation, or came from the catalyst itself (metal oxidation, hydrogen desorption). H_2O experiments followed the same procedure as had been done in the model compound tests, including catalyst reduction *in-situ* and purging with N_2 before the reaction was initiated. The outlet gas concentration of H_2 (vol-%) for H_2O tests in comparison to 4MC runs is shown in Figure 8.

Based on the results from water tests, it seems that at least a part of the detected H_2 in the beginning of the experiment was not formed in the APR-reaction. For example, with NiCu/Al the H_2 outlet concentrations were almost the same in 4MC and H_2O tests (Figure 8), indicating

that hydrogen originates from the catalyst itself. Whereas with Pt/AC and NiCo/ZrO_2 catalyst, there is clearly a portion of H_2 that is formed from reforming reaction. This effect was not visible with methanol APR as the conversion of the reactant and product yields were much higher compared to 4-methylcatechol. Possible explanations for the H_2 formation in the H_2O tests are the Ni re-oxidation with H_2O when water is introduced to the reactor, or desorption of H_2 from the catalyst surface after the reduction. However, to verify this we would need to apply online characterization methods to study the oxidation state of nickel particles, which is not applicable to our setup. Catalyst deactivation with 4MC is further discussed in section **3.4** Error! Reference s ource not found..

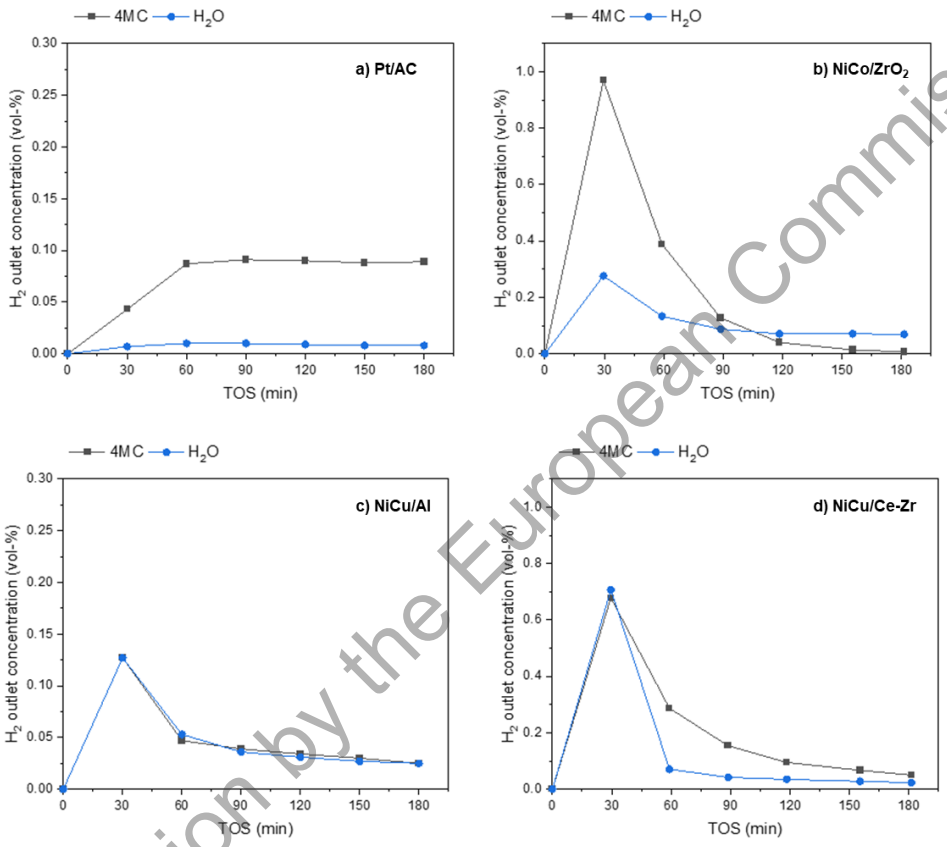

Figure 8. H_2 concentration in the outlet gas with pure H_2O and 4MC tests for different catalysts. Reaction conditions: 32 bar, 230 °C, $Q_{tot,liq.}$= 2 cm^3/min, m_{cat}= 1.5 g, Q(N_2)=75 Ncm^3/min.

3.2.3 Phenol

Phenol was chosen as the second aromatic compound to test for APR. Similarly to 4MC, this compound was tested with Ni, Fe, and Pt catalysts. Fe or Pt did not show any catalytic activity in the conditions tested. Fast catalyst deactivation was also observed with nickel catalysts in the APR of phenol, similar to 4MC runs. Figure 9 shows that there is a rapid incline in H_2 production at TOS=30 min, after which the hydrogen formation decreases to almost zero with NiCu/Al and NiCu/Ce-Zr. Interestingly, the NiCo/ZrO_2 catalyst showed a reasonably and stable H_2 production during the 180 min experimental period; H_2 production was around 15 µmol/min•g_{cat} before the experiment was stopped. Phenol conversion after 180 minutes was calculated to be 1.8% for this catalyst. The long induction period observed with NiCo/ZrO_2 is specific to this catalyst.

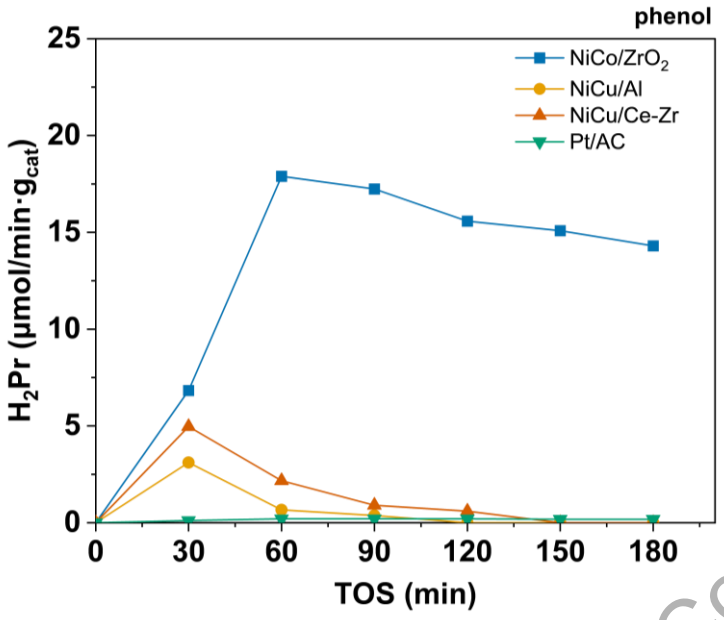

Figure 9. H_2Pr vs. time-on-stream for tested Pt and Ni catalysts in APR of phenol. Reaction conditions: 32 bar, 230 °C, $Q_{tot,liq.}$= 2 cm^3/min (5 wt.% phenol), m_{cat}= 1.5 g, $Q(N_2)$=75 Ncm^3/min.

To understand which reactions take place before the catalyst deactivates, we wanted to compare the product selectivity at TOS=30 min for the phenol runs. For the more stable $NiCo/ZrO_2$, the product selectivity was also assessed at TOS=180 min. The product selectivity for each nickel catalyst can be seen in Figure 10. $NiCo/ZrO_2$ seemed to catalyze both reforming and WGS reaction, as well as hydrogenation of phenol to liquid products. For $NiCo/ZrO_2$, the detected products in the AP were cyclohexanone and cyclohexanol, with cyclohexanone being the dominant product. For ZrO_2 supported nickel, the liquid product selectivity decreased per time-on-stream, from ~18% (TOS=30 min) to 5% (TOS=180 min). At TOS 180, the H_2 and the CO_2 selectivities were 66% and 28%, respectively. For NiCu/Al, we observed only hydrogen and liquid products in the beginning of the reaction, which shortly disappeared after 30 min. In contrast, with NiCu/Ce-Zr catalyst, there was an indication of reforming reactions to occur, which was seen as CO_2 formation in the beginning of the experiment. However, after 90 minutes, CO_2 disappeared from the gaseous product. At the same time, liquid products also disappeared, which is associated with the deactivation of the catalyst.

In the previous experiments with 4MC, we found that fraction of the detected H_2 was not formed during the APR (Figure 8). This behavior was found only for nickel catalyst. When we compared H_2 outlet concentration between phenol and water tests, there was indication that part of the H_2 could be produced from other sources, such as metal reoxidation as reported previously, or by coke formation (phenol condensation over the catalyst).

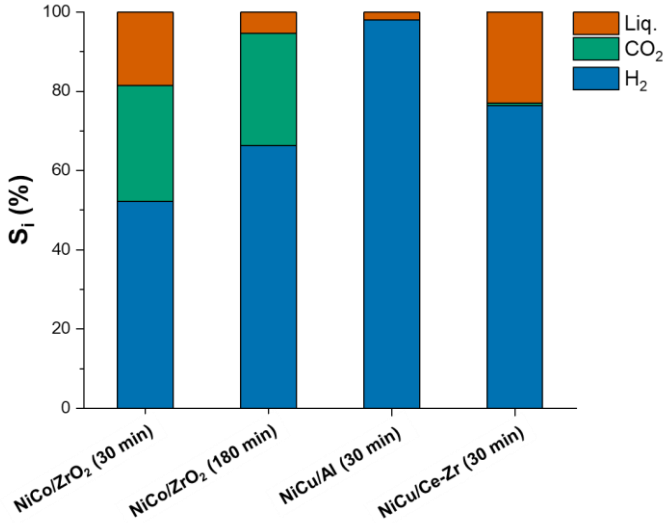

Figure 10. Product selectivity (S_i) for nickel catalysts during phenol APR. Reaction conditions: 32 bar, 230 °C, $Q_{tot,liq.}$= 2 cm^3/min (5 wt.% phenol), m_{cat}= 1.5 g, Q(N_2)=75 Ncm^3/min.

3.2.4 Acetic acid

Acetic acid was chosen to model the group of carboxylic acids found in the aqueous phase of BL processing. Figure 11 displays the conversion of acetic acid over a 3-hour period. All nickel catalysts experienced significant deactivation within the testing period, while Pt/AC catalyst achieved a stable AcOH conversion rate of approximately 10%. The major cause of deactivation in the case of AcOH was attributed to metal leaching (>80% of active metals leached during the experiment), which resulted from the low pH of the solution (Table 1).

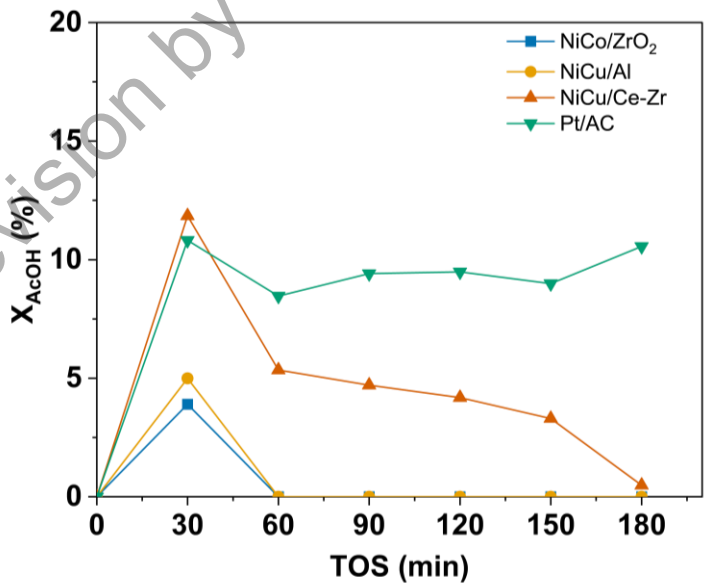

Figure 11. Acetic acid conversion vs. time-on-stream. Reaction conditions: 32 bar, 230 °C, $Q_{tot,liq.}$= 2 cm^3/min (5 wt.% AcOH), m_{cat}= 1.5 g, Q(N_2)=75 Ncm^3/min.

Figure 12 depicts the gas phase selectivity and hydrogen production rate at TOS=3h for AcOH APR. After the three-hour test, only Pt/AC and NiCu/Ce-Zr showed some activity. The H_2 production rate at TOS=3h was 0.7 and 7 µmol/min•g_{cat} for NiCu/Ce-Zr and Pt/AC, respectively. The 10 times higher production rate is linked to the higher AcOH conversion with Pt/AC, as the H_2 selectivity for the catalyst was only few percents, as shown in Figure 12. Moreover, the product selectivity of the two catalysts was found to be very different from each other. We note that no liquid product, other than unreacted acetic acid was found in the withdrawn liquid samples. Based on the measured gas composition, NiCu/Ce-Zr was found to be more prone to catalyze reforming reactions than Pt, with over 80% selectivity to H_2. On the other hand, with Pt/AC, the main reaction products were methane ($S(CH_4)$=52%) and carbon dioxide ($S(CO_2)$=45%), indicating that Pt favours acetic acid decarboxylation reaction under the studied reaction conditions. It should be noted that despite the lower H_2 selectivity, the Pt catalyst showed higher H_2 production rate at the end of the test run compared to nickel catalyst, which correlated with the higher AcOH conversion.

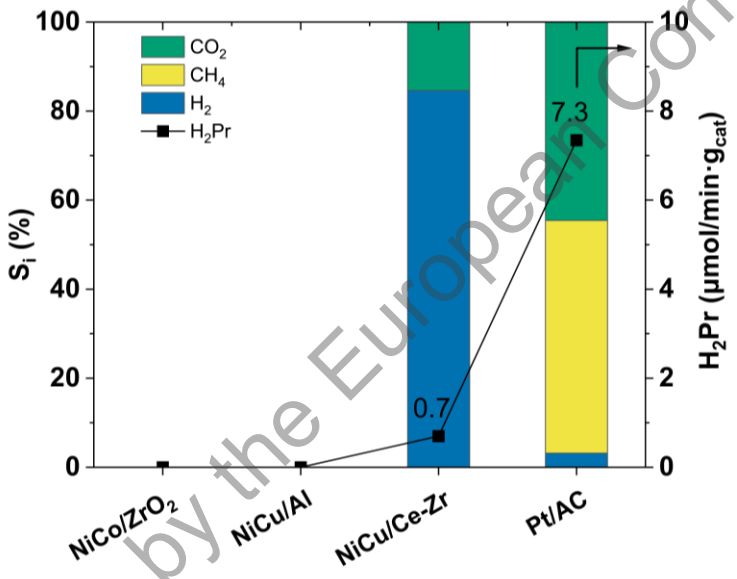

Figure 12. Product selectivity (S_i) and H_2Pr for different catalysts during APR of AcOH. Reaction conditions: 32 bar, 230 °C, $Q_{tot,liq.}$= 2 cm³/min (5 wt.% AcOH), m_{cat}= 1.5 g, Q(N_2)=75 Ncm³/min. Reported values are at TOS= 3h.

3.3 Experiments with 4-component mixture

After studying the model compounds separately, the APR experimental work was completed using a mixture of model compounds to obtain results that mimic the real process waters. Tests were conducted using a 4-component mixture (MIX-4) and the two best catalysts, Pt/AC and $NiCo/ZrO_2$, which were selected based on the results from the APR experiments with 1-component solutions. The experiments were carried out under the same reaction conditions as in the screening with 1-component feed, and the experimental period was extended to 8 hours to compare the long-term stability and activity of the catalysts.

Figure 13 shows the reactant conversions for Pt/AC and $NiCo/ZrO_2$ catalysts during APR of MIX-4. As expected, the Pt catalyst was found to be more stable than nickel. With $NiCo/ZrO_2$, the conversion of reactants peaked at the beginning of the experiment and decreased constantly during operation. The most significant decrease was seen in the conversion of 4MC,

which fell from 15% to below 5% within the first 60 minutes of TOS. There was also some variation in reactant conversion values during 8-hour testing period for Ni catalyst, possibly due to technical problems with the isocratic pump during the experimental run. Pt/AC showed reasonably stable conversion for phenol and methanol throughout the 8-hour experiment. Whereas for 4MC, the conversion decreases from ~60% to 40% during the experimental period. Interestingly, AcOH showed negative conversion with MIX-4 tests when tested with Pt/AC. The negative conversion for AcOH could be explained by reverse decarboxylation reaction of CH_4 and CO_2 to form more acetic acid, identified from the 1-component experiment.

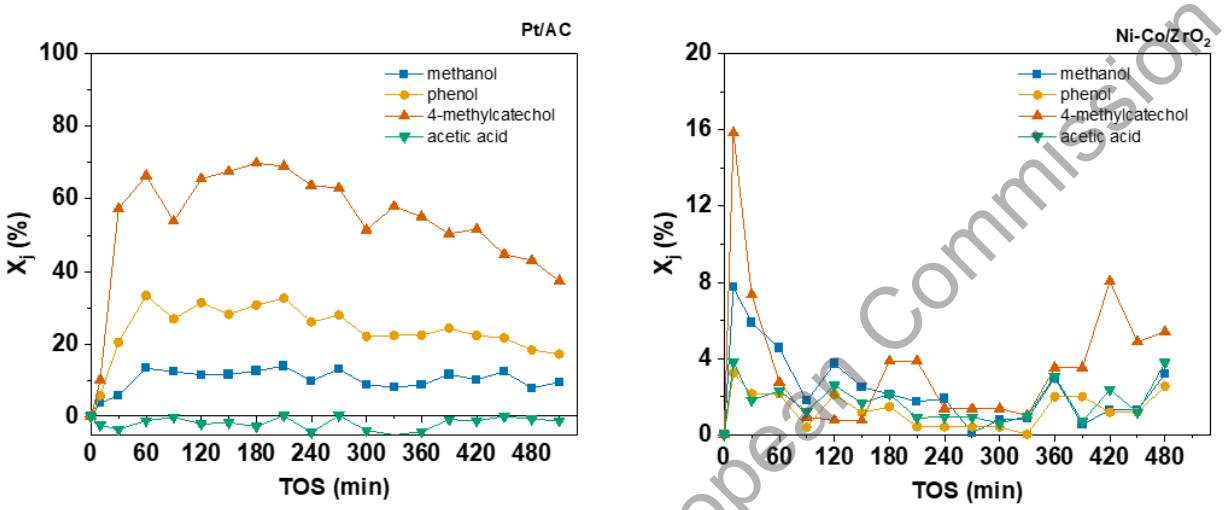

Figure 13. Conversion of each model compound during APR of MIX-4. Left: Pt/AC and Right: NiCo/ZrO_2. Reaction conditions: 32 bar, 230 °C, $Q_{tot,liq.}$= 2 cm^3/min (2.5 wt.% of MeOH, AcOH, phenol, and 4MC), m_{cat}= 1.5 g, Q(N_2)=75 Ncm^3/min.

Figure 14 shows the product selectivity over the two catalysts. For comparison purposes, product selectivity at TOS 180 and 480 minutes have been included in the same figure. This enabled us to assess the reactions that occur with the simulated mixture and to compare the product selectivity to 1-component feed after 3 hours. For both catalysts, the product selectivity remained quite stable during the 8-hour testing period despite the decrease of conversion of some of the reactants. Similar to the experiments with oxygenated aromatics, the Pt catalyst was found to be more selective to liquid products than Ni. With Nickel catalyst, the H_2 selectivity was around 80% at 180 and 480 min time-on stream. However, CH_4 (5.7 vol.%), CO (1.7 vol.%), and HCs (0.2 vol.%) were also formed during the first 60 minutes, and they disappeared as the catalyst deactivated. With Pt, the main liquid products were *m*-cresol, *p*-cresol and cyclohexanone. Additionally, there were also smaller peaks of cyclohexanol detected in some of the liquid samples. We note that the carbon balance closure was 90 – 94% for Pt/AC catalyst. The missing carbon could be explained partially by the formation of new liquid products that were not quantified due to their low concentration compared to the main liquid products, or by coke deposition on the catalyst.

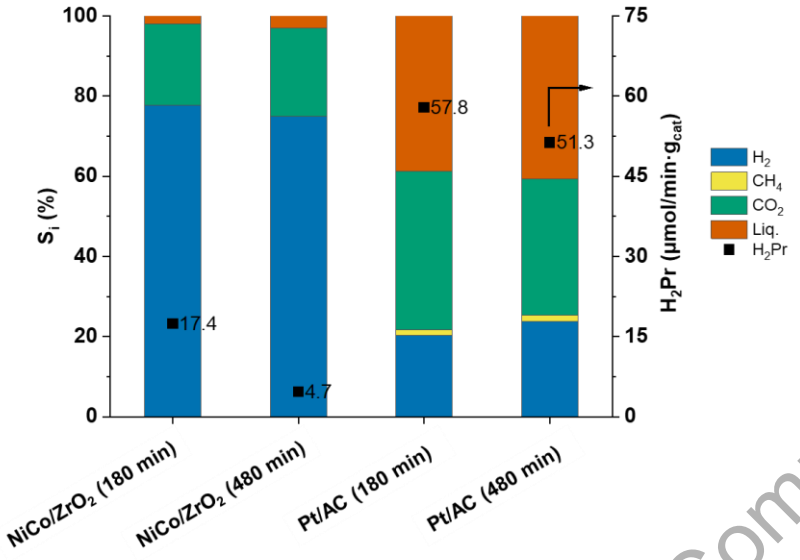

Figure 14. Product selectivity (S_i) and H_2Pr for NiCo/ZrO_2 and Pt/AC catalyst during APR of MIX-4. Reaction conditions: 32 bar, 230 °C, $Q_{tot,liq.}$ = 2 cm^3/min (2.5 wt.% of MeOH, AcOH, phenol and 4MC), m_{cat} = 1.5 g, Q(N_2)=75 Ncm^3/min.

3.4 Characterization of spent catalysts

To gain insight into the deactivation during the APR experiments, the catalysts were thoroughly characterized after the experiments. The focus was on the nickel catalysts, which showed severe deactivation during the experiments. Ru and Fe catalysts were excluded from the analyses due to their poorer activity for APR. The spent catalysts were characterized for their metal content (ICP-OES), textural properties (N_2 physisorption), XRD, and carbon content (C analysis). Data from the characterizations was compared against data of the fresh catalysts. When available, data for Pt catalysts is included.

ICP-OES

ICP-OES analysis was conducted to evaluate metal leaching. Table 6 shows the percentage of metal loss after the APR reaction compared to the metal content in the calcined sample. Among all the tested catalysts, NiCu/Ce-Zr was the most resistant to metal leaching. This catalyst showed no leaching of either nickel or promoter with methanol or phenol experiments.

Along with the support, the ICP results indicated that the choice of promoter could affect the observed Ni and promoter leaching. Co-doped catalysts were found to be more sensitive to leaching than Cu-promoted nickel. The stability of the metal phases formed during catalyst calcination and reduction could explain this difference.

Metal leaching is typical for acidic solutions and is more pronounced in hydrothermal conditions like those used in this study. The most evident metal leaching occurred with nickel catalysts tested for AcOH APR, which was the most acidic solution (pH 2.5, Table 1). More than 80% of the nickel had been leached with AcOH, regardless of the catalyst used. Among the three nickel catalysts tested, NiCo/ZrO_2 was the least stable, resulting in more than 99% of the nickel leaching during the tests. After the AcOH experiment, the NiCo/ZrO_2 catalyst sample was withdrawn from the reactor, and the white catalyst support was exposed due to metal leaching,

as seen in Figure 15. In contrast, MeOH, the most neutral solution with a pH of 6.7, resulted in the least leaching of metal or promoter compared to other model compounds or their mixture.

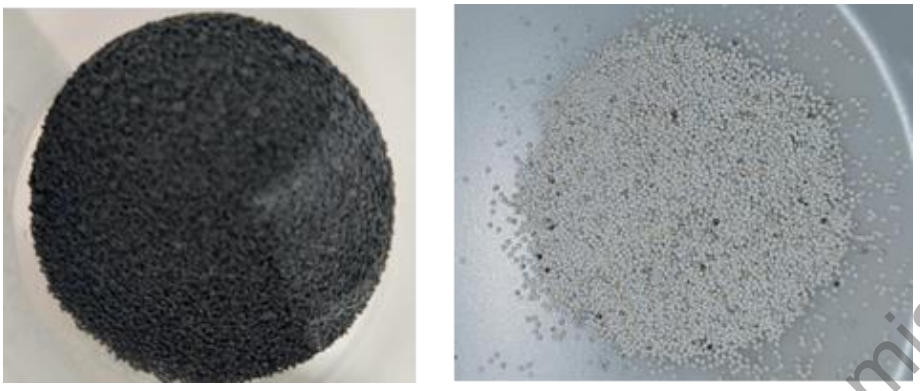

Figure 15. Left hand side: picture of the calcined $NiCo/ZrO_2$ catalyst. Right hand side: picture of the $NiCo/ZrO_2$ catalyst after APR experiments with 5 wt.% AcOH.

Table 6. Results of the ICP-OES analysis for nickel catalysts

Catalyst	Composition	Component	Leached Ni, %	Leached Co, %	Leached Cu, %
NiCu/Ce-Zr	10%Ni–5%Cu/Ce-Zr	MeOH	-		-
		phenol	-		-
		4MC	8.4		8.4
		AcOH	91.0		91.0
NiCu/Al	10%Ni–10%Cu/γ-Al_2O_3	MeOH	3.8		3.2
		phenol	9.3		8.5
		4MC	9.3		8.3
		AcOH	79.9		9.2
$NiCo/ZrO_2$	10%Ni–5%Co/ZrO_2	MeOH	1.8	1.6	
		phenol	3.3	13.2	
		4MC	19.0	27.0	
		AcOH	99.5	99.6	
		MIX-4	92.8	97.3	

Nitrogen adsorption-desorption

N_2 physisorption was used to follow the changes in catalyst BET surface areas, pore volumes and pore diameters. Table 7 contains adsorption-desorption data for calcined and spent catalyst samples. We also characterized catalysts that were subjected to H_2O tests. Their results are included in the table.

Based on the N_2 physisorption data, the NiCu/Ce-Zr catalyst appears the most stable among all the tested Ni and Pt catalysts. There were no significant changes observed in the BET surface

area, pore volume, or pore diameter in any of the tests, except for NiCu/Ce-Zr exposed to 4MC, where there was a slight decrease in all these characteristics. A more pronounced decrease was observed for all catalysts tested in 4MC aqueous phase reforming. This is expected to be due to the accumulation of carbon species on the catalyst surface (dilution effect) that blocked the catalyst's active sites, which in turn could explain the overall lower activity of 4MC for APR. To verify the hypothesis on carbon formation, we measured the carbon content of the calcined and spent catalysts. The results are presented and discussed in the section **Carbon content analysis**.

NiCu/Al was found to be the least stable catalyst. Even with pure H_2O, there was a decrease in the surface area and pore volume indicating the collapse or structural changes of the alumina support. Further XRD analysis revealed the phase change of alumina to boehmite, which explains the observed behavior. With NiCu/Al catalyst and acetic acid, there was also a significant increase in pore diameter. In these reaction conditions, acetic acid could work as etching agent, therefore changing the morphology of the catalyst. The same increase in surface area, pore volume, and diameter was seen also with other nickel catalysts, while the effect is not as pronounced as with NiCu/Al.

Table 7. N_2 physisorption data for fresh and spent nickel catalysts. Data from N_2 desorption isotherm

Sample		S_{BET} (m^2/g)	Pore volume BJH (cm^3/g)	Average pore diameter by BET (nm)
NiCu/Ce-Zr	calcined	88	0.19	7
	MeOH	92	0.21	8
	4MC	76	0.12	6
	phenol	88	0.19	8
	AcOH	96	0.22	8
	H_2O	88	0.19	8
NiCu/Al	calcined	184	0.53	10
	MeOH	18	0.09	11
	4MC	153	0.33	8
	phenol	74	0.18	9
	AcOH	46	0.39	32
	H_2O	80	0.24	12
$NiCo/ZrO_2$	calcined	63	0.23	11
	MeOH	63	0.24	11
	4MC	54	0.15	10
	phenol	62	0.18	11
	AcOH	75	0.26	11
	MIX-4	78	0.23	10
	H_2O	73	0.24	11
Pt/AC	calcined	915	0.43	5
	MeOH	847	0.41	5
	4MC	516	0.34	5
	phenol	757	0.39	5
	AcOH	916	0.42	5
	MIX-4	411	0.34	5
	H_2O	860	0.41	5

XRD analysis

XRD analysis was conducted for calcined, reduced, and spent nickel catalysts to evaluate further morphological changes and crystallite growth. Catalysts tested with solutions containing acetic acid were not analyzed with XRD as more than 80 % of the active metals had been leached during the experiment making the analysis inconclusive.

Based on the XRD analysis, metastable alumina (Al) support was found to change phase from γ-Al_2O_3 to boehmite (γ-AlO(OH)) under tested reaction conditions for phenol and methanol APR. Interestingly, a similar change was not observed with NiCu/Al tested with 4MC. Compared to Al support, Ce-Zr and ZrO_2 were more stable and no obvious change in catalyst morphology was observed with any of the samples, which is in line with results from N_2 adsorption-desorption. Table 8 shows the crystal size of the alloy (for reduced state and spent catalyst) calculated with the Scherrer equation (Eq. 1). In general, the crystal particle size was increased for the catalysts tested with oxygenated aromatics when compared to the size of the reduced particles. In particular, the change in the crystal form of Al to boehmite seems to cause a change in the catalyst when the structure breaks down, therefore increasing the probability of the active metal crystal growth. Samples tested in methanol APR were found to maintain their original crystallite size after the experiments except for NiCu/Ce-Zr, which showed smaller crystal size after the test run.

Table 8. Mixed alloy crystal size calculated from X-ray diffractograms

Sample		$d_{mixed\ alloy}$ (nm)
NiCu/Ce-Zr	reduced	27
	MeOH	17
	4MC	25
	phenol	22
NiCu/Al	reduced	18
	MeOH	15
	4MC	50
	phenol	40
NiCo/ZrO_2	reduced	17
	MeOH	19
	4MC	31
	phenol	28

Carbon content analysis

Our study included C analyses on both calcined and spent Ni-catalysts to identify if carbon-based fouling was responsible for the catalyst deactivation observed with aromatic compounds. In particular, with 4MC runs, a decrease of the average pore diameter was shown with N_2 physisorption measurements (Table 6). The carbon content was analyzed by burning

the sample in pure O_2 at 950 °C. The measured C-contents for calcined and spent catalysts are presented in Table 9.

As seen from the table, also calcined catalyst samples contained a small amount of residual carbon. This could be attributed to some residual graphitic carbon from the support synthesis, or from the adsorption of carbonate on the calcined material. The measured C concentration for calcined samples was 0.4 wt.% or lower, for all catalysts. When MeOH was used, the measured carbon content was found to be almost the same or lower as that of calcined catalysts. The small deviation could be put into the error margin of the analysis. For phenol, there was a slight increase (≤0.6 wt.%) in the value. Further analysis of the liquid products revealed that phenol polymerization was taking place, which resulted in the formation of a dimer, o-hydroxybiphenol. Even a small amount of these larger molecules could potentially block the active sites of the tested catalysts and cause deactivation during the APR of phenol. However, for 4MC and the experiment with a 4-component mixture, there is a clear increase in the measured carbon content (up to ~10%), which supports the results from N_2 physisorption and explains the lower activity and the faster deactivation of the catalysts in the 4MC APR runs.

Table 9. Detected carbon content (wt.%) in calcined and spent Ni catalysts

Sample	NiCu/Ce-Zr	NiCu/Al	NiCo/ZrO_2
	wt.%	wt.%	wt.%
calcined	0.3	0.4	0.4
MeOH	0.3	0.1	0.2
phenol	0.9	0.5	0.8
4MC	7.2	7.1	10.2
AcOH	1.6	0.8	1.1
MIX-4	-	-	3.1

(-) = not tested for APR of MIX-4.

4 Summary and future prospects

The objective of Task 2.3 was to study the aqueous phase reforming of the aqueous phase obtained from black liquor HTL processing to produce hydrogen for the BL2F process. The work involved extensive catalyst screening with four individual model compounds, followed by eight-hour experiments with a 4-component mixture using the best catalysts selected from the catalyst screening. The used model compounds for this work were methanol, acetic acid, phenol, and 4-methylcatechol, which were selected based on the analysis of the samples produced from the HTL of BL in batch reactor, performed by KIT in WP1. The catalysts tested included Ni and Fe-based catalysts prepared by VTT, and commercial catalysts such as Ru/AC and Pt/AC. All experiments were conducted under the same conditions, with only the model compound mixture and time-on-stream used as variables.

Out of the tested individual model compounds, methanol yielded the best H_2 selectivity (~70%) and a stable H_2 production rate of ~620 µmol/min•g_{cat} (Y(H_2) = 32%) with both, nickel and platinum catalysts. Whereas with the other compounds: acetic acid, 4-methylcatechol, and phenol, the nickel catalysts lost significant amount of their initial activity within the first 60 minutes of time-on-stream. Two best catalysts, Pt/AC and NiCo/ZrO_2, were selected for long-term tests with the 4-component solutions. Out of the two catalysts, Pt was found to be more stable than nickel, similar to the observations made in the experiments with individual model compounds. After 8h-experiment with 4-component solution, the H_2 production rate with Pt had decreased only by ~11% of the initial value (from 57 to 51 µmol/min•g_{cat}), as for Ni, the decrease was ca. 95% (from 100 to 5 µmol/min•g_{cat}). The main causes of Ni catalysts deactivation were found to be the metal leaching and/or the blockage of the active sites due to coking, i.e., accumulation of carbon species over the catalyst surface formed by the polymerization of aromatic compounds (a dimer was identified).

Despite their lower stability, nickel catalysts were found to be more selective towards hydrogen than noble metals. Pt showed more stable activity over a long period of time but had a higher liquid product selectivity when tested with oxygenated aromatics. Based on the analysis of the product phases, Pt seems to promote not only hydrodeoxygenation and hydrogenation reaction with aromatic compounds, but also decarboxylation with acetic acid. As a consequence, the H_2 produced is consumed within undesired side reactions, thus lowering the overall hydrogen production and the selectivity of the catalyst.

To summarize, the H_2 yield reached during all carried out tests was surprisingly low, even with the best case, i.e., methanol APR. When comparing the experimental results of this work with the model of large scale BL2F plant created in T4.2 (D4.2, SINTEF), we could conclude that the H_2 yield from the APR of BL water is insufficient for an industrially relevant scale. An additional supply of hydrogen would be required in order to meet the H_2 demand of the HDO steps. Additionally, nickel catalysts would be more suitable for larger concept due to their good H_2 selectivity. However, using a nickel catalyst in a relevant scale would need an additional extensive catalyst development to improve their hydrothermal stability and endurance in the long run. The resistance of the catalysts towards leaching is not the main concern as real aqueous phases produced from HTL equipped with salt separation should have higher pH (above 7). The next proposed studies should then focus on stability of the best catalysts towards leaching with real aqueous phases. The effects of pH and remaining salts in the AP originating from HTL is to be further studied and verified. It was not in the scope of this project to go into a deep analysis of all the details observed in catalyst behavior (e.g. reaction networks)

or catalyst characterizations. These will be considered in following up studies. The results of this work form a solid basis for at least two scientific publications, which will be written and will lead to a doctoral thesis within the coming three years.

5 Bibliography

Baudouin, D., Xiang, H., & Vogel, F. (2022). On the selective desulphurization of biomass derivatives in supercritical water. *Biomass and Bioenergy*, *164*. https://doi.org/10.1016/j.biombioe.2022.106529

Coronado, I., Pitínová, M., Karinen, R., Reinikainen, M., Puurunen, R. L., & Lehtonen, J. (2018). Aqueous-phase reforming of Fischer-Tropsch alcohols over nickel-based catalysts to produce hydrogen: Product distribution and reaction pathways. *Applied Catalysis A: General*, *567*(September), 112–121. https://doi.org/10.1016/j.apcata.2018.09.013

Davda, R. R., Shabaker, J. W., Huber, G. W., Cortright, R. D., & Dumesic, J. A. (2003). Aqueous-phase reforming of ethylene glycol on silica-supported metal catalysts. *Applied Catalysis B: Environmental*, *43*(1), 13–26. https://doi.org/10.1016/S0926-3373(02)00277-1

Pipitone, G., Zoppi, G., Pirone, R., & Bensaid, S. (2022). A critical review on catalyst design for aqueous phase reforming. *International Journal of Hydrogen Energy*, *47*(1), 151–180. https://doi.org/10.1016/j.ijhydene.2021.09.206